The Journal of Immunology

Mitochondrial Structural Changes and Dysfunction Are Associated with Experimental Allergic Asthma

Ulaganathan Mabalirajan, Amit Kumar Dinda, Sarvesh Kumar, Reema Roshan, Pooja Gupta, Surendra Kumar Sharma and Balaram Ghosh

J Immunol 2008; 181:3540-3548; ;
doi: 10.4049/jimmunol.181.5.3540
http://www.jimmunol.org/content/181/5/3540

The Journal of Immunology is published twice each month by
The American Association of Immunologists, Inc.,
1451 Rockville Pike, Suite 650, Rockville, MD 20852

Print ISSN: 0022-1767 Online ISSN: 1550-6606.

Mitochondrial Structural Changes and Dysfunction Are Associated with Experimental Allergic Asthma[1]

Ulaganathan Mabalirajan,*‡ Amit Kumar Dinda,† Sarvesh Kumar,* Reema Roshan,* Pooja Gupta,* Surendra Kumar Sharma,‡ and Balaram Ghosh[2]*

An imbalance between Th1 and Th2 immune response is crucial for the development of pathophysiological features of asthma. A Th2-dominant response produces oxidative stress in the airways, and it is thought to be one of the crucial components of asthma pathogenesis. Although mitochondrion is a crucial organelle to produce endogenous reactive oxygen species, its involvement in this process remains unexplored as yet. We demonstrate in this study that OVA-induced experimental allergic asthma in BALB/c mice is associated with mitochondrial dysfunction, such as reduction of cytochrome *c* oxidase activity in lung mitochondria, reduction in the expression of subunit III of cytochrome *c* oxidase in bronchial epithelium, appearance of cytochrome *c* in the lung cytosol, decreased lung ATP levels, reduction in the expression of 17 kDa of complex I in bronchial epithelium, and mitochondrial ultrastructural changes such as loss of cristae and swelling. However, there was no change in the expression of subunits II and III of cytochrome *c* oxidase. Interestingly, administration of IL-4 mAb reversed these mitochondrial dysfunction and structural changes. In contrast, IFN-γ mAb administration neither reversed nor further deteriorated the mitochondrial dysfunction and structural changes compared with control asthmatic mice administered with isotypic control Ab, although airway hyperresponsiveness deteriorated further. These results suggest that mitochondrial structural changes and dysfunction are associated with allergic asthma. These findings may help in the development of novel drug molecules targeting mitochondria for the treatment of asthma. ***The Journal of Immunology,*** **2008, 181: 3540–3548.**

Allergic asthma is mediated by dominant Th2 immune response and characterized by airway hyperresponsiveness (AHR),[3] airway inflammation, increased IgE levels, and mucus hypersecretion. IL-4 especially is required for differentiation of naive T cells to Th2 phenotype, and it is involved in many critical pathobiological mechanisms, including epithelial injury and mucus secretion (1). Allergen exposure induces acquired and innate immune systems to release proinflammatory mediators like histamine, PGs, and leukotrienes, which lead to recruitment and activation of various inflammatory cells, such as mast cells, eosinophils, neutrophils, lymphocytes, macrophages, and platelets (2). These recruited cells release various reactive free radicals such as superoxide anion, hydroxyl radicals, hydrogen peroxide, NO, peroxynitrite, etc., by enzymes of many oxidative pathways, such as eosinophil peroxidase and myeloperoxidase. These free radicals leak into the surrounding cells of the airway and create a local oxidative milieu (2). This oxidative microenvironment causes damage and injury to airway epithelial cells, leading to loss of epithelium from the basement membrane (2).

Moreover, asthmatic epithelium has abnormal susceptibility for oxidant-induced damage and apoptosis compared with normal epithelium due to the reduction in the endogenous epithelial protective factors, such as heat shock protein 27, labile Zn, superoxide dismutase, and/or intake of exogenous diets low in antioxidants (3–5). In addition, increased numbers of mitochondria and altered mitochondria have been observed in bronchial epithelium in murine model of asthma and asthmatic children (6, 7). Also, oxidative-free radicals relevant to asthma pathogenesis, such as peroxynitrite, primarily affect cytochrome *c* oxidase by degrading its heme centers and damaging its copper center. Cytochrome *c* oxidase of electron transport chain (COX_{ETC}) is a key oxidative enzyme in mitochondria (8). COX_{ETC} catalyzes the electron transfer to generate ATP via the coupled process of oxidative phosphorylation and consumes most cellular oxygen (9). The inhibition of COX_{ETC} has been reported to cause oxidative stress and initiation of mitochondrial-mediated apoptosis (10). Among 13 subunits of COX_{ETC}, its catalytic activity is primarily determined by three subunits, which are all encoded by mitochondria (9). Oxidative insults specifically affect the third subunit of COX_{ETC}, which is essential for the stabilization of the entire complex (11). However, the exact role of mitochondria in this context is not yet elucidated, although mitochondrion is one of the major sources of endogenous reactive oxygen species. It has been hypothesized that IL-4-induced apoptosis is the major cause for denudation of airway epithelium and other inflammatory changes in asthma (12). In view of these roles of mitochondria, we hypothesized that IL-4 could be associated with mitochondrial dysfunction in asthma pathogenesis.

*Molecular Immunogenetics Laboratory, Institute of Genomics and Integrative Biology, Delhi, India; and †Division of Renal Pathology, Department of Pathology, and ‡Division of Pulmonary, Critical Care and Sleep Medicine, Department of Medicine, All India Institute of Medical Sciences, Ansari Nagar, New Delhi, India

Received for publication December 18, 2007. Accepted for publication June 23, 2008.

The costs of publication of this article were defrayed in part by the payment of page charges. This article must therefore be hereby marked *advertisement* in accordance with 18 U.S.C. Section 1734 solely to indicate this fact.

[1] This work was supported by the Net Work Project (NWP0033) of Council of Scientific and Industrial Research (Government of India) and Task Force Project SMM0006 of Council of Scientific and Industrial Research (Government of India). U.M. was supported by a fellowship from the Indian Council of Medical Research.

[2] Address correspondence and reprint requests to Dr. Balaram Ghosh, Molecular Immunogenetics Laboratory, Institute of Genomics and Integrative Biology, Mall Road, Delhi-110007. E-mail address: bghosh@igib.res.in

[3] Abbreviations used in this paper: AHR, airway hyperresponsiveness; A.CON, asthmatic control; BAL, bronchoalveolar lavage; COX_{ETC}, cytochrome *c* oxidase of electron transport chain; CYTO, cytosolic fraction; DCP, double-chamber plethysmography; DEX, dexamethasone; HODE, hydroxyoctadecaenoic acid; IHC, immunohistochemistry; L-OOH, lipid hydroperoxide; MCh, methacholine; N.CON, normal control; Penh, enhanced pause; SCP, single-chamber plethysmography; sGaw, specific airway conductance; sRaw, specific airway resistance; ISO, isotypic.

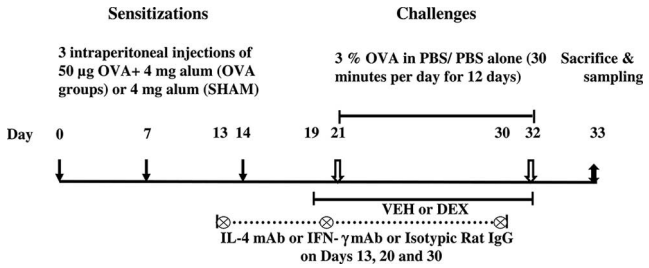

FIGURE 1. Experimental protocol for the induction of allergic asthma. Eight- to 10-wk-old male BALB/c were grouped, sensitized, and challenged, as described in *Materials and Methods*. Vehicle (DMSO) or DEX has been given orally from days 19 to 32. Normal rat IgG, IL-4 mAb, or IFN-γ mAb was administered to respective groups i.p. on days 13, 20, and 30. AHR measurement and sacrifice were performed on day 33.

To understand this, we have checked ultrastructural changes of mitochondria of bronchial epithelium and several key functions of lung mitochondria related to COX_{ETC} in asthmatic mice administered with either IL-4 mAb or IFN-γ mAb. In this study, we have shown that mitochondrial damage and alterations of its key functions are associated with experimental allergic asthma.

Materials and Methods

Animals

Male BALB/c mice (8–10 wk old) were obtained from National Institute of Nutrition (Hyderabad, India) and acclimatized for 1 wk prior to starting the experiments. All animals were maintained as per Committee for the Purpose of Control and Supervision of Experiments on Animals guidelines, and protocols were approved by Institutional Animal Ethics Committee.

Grouping of mice

Mice were divided into five groups, and each group was named according to sensitization/challenge/treatment, as follows: SHAM/PBS/normal controls (N.CON), OVA/OVA/asthmatic controls (A.CON) (OVA, chicken egg OVA, grade V; Sigma-Aldrich), OVA/OVA/dexamethasone (DEX) (Sigma-Aldrich; $n = 6$ mice), OVA/OVA/IL-4 mAb (mAb against murine IL-4; R&D Systems; $n = 6$ mice), and OVA/OVA/IFN-γ mAb (mAb against murine IFN-γ; R&D Systems; $n = 6$ mice). SHAM/PBS/N.CON represented mice pooled from two subgroups (six mice in each subgroup) treated with either oral DMSO or i.p. injection of PBS. OVA/OVA/A.CON mice also were pool of two subgroups (six mice in each subgroup) treated with either DMSO or i.p. injection of rat IgG as isotypic (ISO) control Ab (OVA/OVA/ISO).

Sensitization, challenge, and treatment of mice

As shown in Fig. 1, mice were sensitized by three i.p. injections of 50 μg of OVA in 4 mg of aluminum hydroxide (OVA groups such as OVA/OVA/A.CON, OVA/OVA/DEX, OVA/OVA/IL-4 mAb, and OVA/OVA/IFN-γ mAb) or 4 mg of aluminum hydroxide (SHAM/PBS/N.CON) on days 0, 7, and 14. Mice were challenged from days 21 to 32 (30 min per day) with 3% OVA in PBS (OVA groups) or PBS (SHAM/PBS/N.CON) using a nebulizer with a flow rate of 9 L/min (OMRON CX3 model). DMSO or DEX (0.75 mg/kg) had been given orally from days 19 to 32 once per day in 10 μl vol per dose. Normal rat IgG, IL-4 mAb, or IFN-γ mAb in 200 μl vol was administered i.p. on days 13 (250 μg), 20 (250 μg), and 30 (125 μg). For determining the adequate dosage of the IL-4 mAb or IFN-γ mAb, initial experiments were performed with different concentrations of the respective Abs (250, 500, and 1000 μg); we determined the efficacy of the Ab treatment by measuring IL-4 or IFN-γ levels in lung tissue homogenates, and the minimum effective dose (250 μg) was selected (data not shown). We selected i.p. route because i.p. injections of IL-4 Ab have been shown to alleviate the asthma features (13).

AHR measurement

AHR to methacholine (MCh; Sigma-Aldrich) was determined in unrestrained and restrained conscious mice by single-chamber plethysmography (SCP) and double-chamber plethysmography (DCP), respectively (model PLY 3211 and PLY 4451; Buxco Electronics), as described previously (14–16). SCP was performed for the estimation of enhanced pause (Penh), and DCP was for the estimation of both specific airway conductance (sGaw) and specific airway resistance (sRaw). We have taken two mice at a time for the measurement either in SCP or in DCP. Totals of 50 μl of PBS/each MCh dose with 15% duty cycle for SCP and 100 μl of PBS/each MCh dose with 30% duty cycle for the DCP have been applied. These variations in dose-volume and instrument setup for SCP and DCP methods might produce variation in dose-response curve. It has been reported that lung resistance strongly correlates with Penh in BALB/c mice (17). Penh has been shown to be useful and reliable in BALB/c mouse model of asthma in which predominant AHR is due to peribronchial inflammation rather than parenchymal inflammation compared with other strains (18). Also, restrained DCP technique has been performed, because this technique is soundly based on the first principles of physics of the lung similar to invasive techniques and allows nonterminal measurements. It has recently been shown that there was an excellent correlation between sRaw-DCP method and airway resistance by the forced oscillation technique (19). These measurements were estimated on day 33 for all mice. Final results

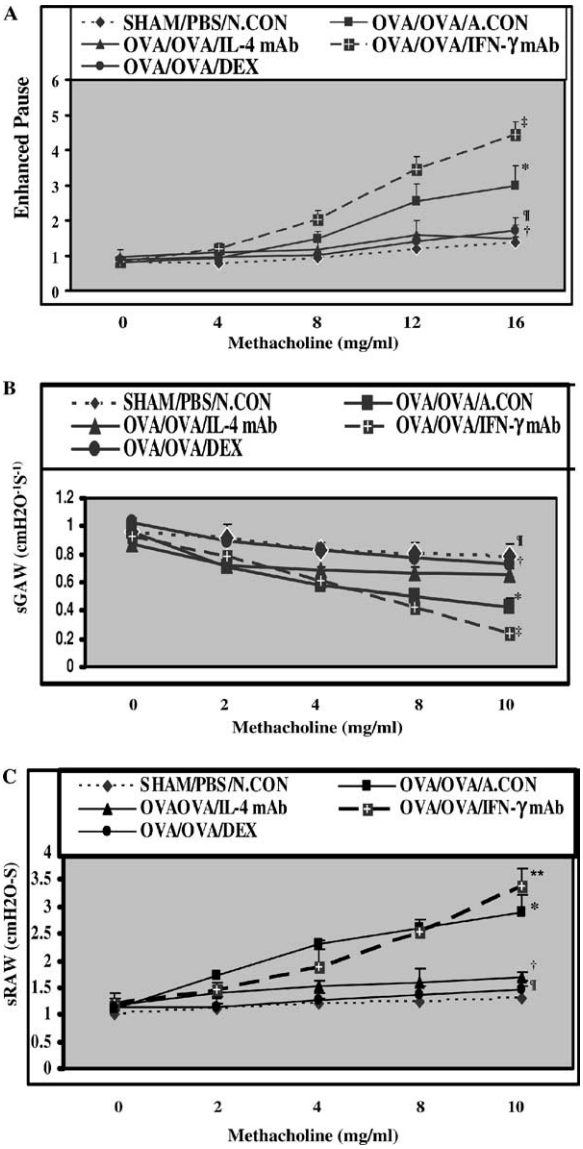

FIGURE 2. Effect of IL-4 mAb or IFN-γ mAb on AHR to MCh. Mice were randomly divided and named as per status of sensitization/challenge/treatment. AHRs were determined on day 33. *A*, Absolute values of Penh (unitless parameter) with increasing concentrations of MCh were estimated. *, $p < 0.05$ vs SHAM/PBS/N.CON; †, ‡, and ¶, $p < 0.05$ vs OVA/OVA/A.CON. *B* and *C*, Absolute values of sGaw and sRaw with increasing concentrations of MCh were estimated. *, $p < 0.05$ vs SHAM/PBS/N.CON; †, ‡, and ¶, $p < 0.05$; and **, NS vs OVA/OVA/A.CON.

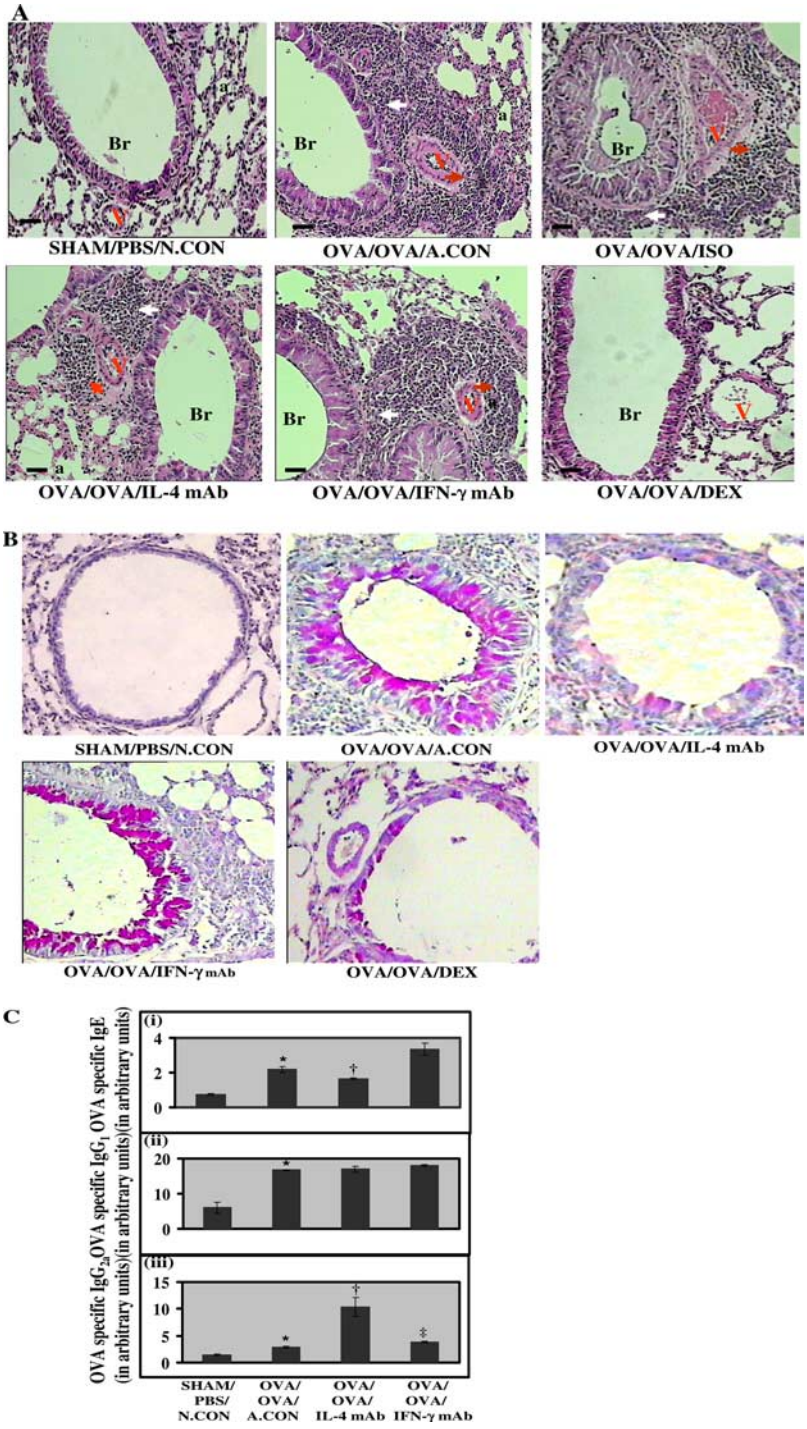

FIGURE 3. Effect of IL-4 mAb or IFN-γ mAb on airway inflammation, goblet cell metaplasia, and OVA-specific IgE, IgG1, and IgG2a levels. *A*, Representative photographs of H&E staining were shown. Br, bronchus; V, vessel; a, alveolus; red arrows indicate the perivascular inflammation; and white arrows indicate the peribronchial inflammation. OVA/OVA/ISO indicates OVA-sensitized and challenged mice administered with isotypic control Ab. Bars, 50 μm. *B*, Representative photographs of periodic acid Schiff staining were shown. Black arrows indicate the goblet cell metaplasia. Bars, 50 μm. *C*, OVA-specific IgE (*i*), IgG1 (*ii*), and IgG2a (*iii*) were estimated in sera, as described in *Materials and Methods*. $*$, $p < 0.05$ vs SHAM/PBS/N.CON; †, $p < 0.05$; and ‡, NS vs OVA/OVA/A.CON.

for SCP were expressed in absolute Penh (unitless) values with each concentration of MCh. For sGaw and sRaw, measurements were performed with increasing concentrations of MCh, and results were expressed in absolute values (cm H_2O^{-1} s^{-1} and cm H_2O-s, respectively).

Bronchoalveolar lavage (BAL) and sera separation

On day 33, each mouse was sacrificed, BAL was performed, and BAL fluids were processed to separate cell pellets and supernatants, as described earlier (20). Briefly, collected BAL fluid was centrifuged at 1000 rpm, for 10 min at 4°C. The cell pellets were washed three times with PBS and resuspended in PBS; a small portion was taken to evaluate total cell number; and differential counts were estimated after staining with Leishman's stain (20). The absolute number of cells was calculated by multiplying the percentage of each subset in an individual sample by the total number of cells in that sample. Blood was withdrawn by cardiac puncture, and serum was separated, as described previously (20).

Combined in situ perfusion and immersion fixation for transmission electron microscopy

Whole body fixation was performed at room temperature, as described earlier (21). Lungs were removed and immersed again in the fixative. The fixed lungs were dissected under dissection microscope (SZX-12; Olympus) to locate the first generation bronchi, and those were cut into many slices of same thickness. Each slice was made into three blocks, and they were further processed; the stained sections were viewed under transmission electron microscope, as described previously (22).

Table I. *Effects of IL-4 mAb, IFN-γ mAb, and DEX on perivascular (PV), peribronchial (PB), total lung inflammation scores, airway mucin content, bronchial epithelial thickness (BET), L-OOH, and 13-S-HODE levels*

	Inflammation Score			Airway Mucin Content (nl/mm^2)	BET (μm)	Lipid H_2O_2 (nm/25 mg lung)	13-S-HODE (ng/50 μg protein)
	PV	PB	Total				
SHAM/PBS/N.CON				1.0 ± 0.2	7.3 ± 1.0	0.55 ± 0.06	85.1 ± 8.2
OVA/OVA/A.CON	2.9 ± 0.2	3.5 ± 0.2	6.4 ± 0.4	13.7 ± 0.7[a]	17.5 ± 1.0[a]	0.84 ± 0.04[a]	119.8 ± 10.5[a]
OVA/OVA/IL-4 mAb	0.8 ± 0.2	1.8 ± 0.4	2.5 ± 0.6[b]	2.9 ± 0.3[b]	7.5 ± 1.0[b]	0.55 ± 0.10[b]	99.9 ± 11.3[b]
OVA/OVA/IFN-γ mAb	3.1 ± 0.07	3.1 ± 0.2	6.2 ± 0.2	16.8 ± 1.6	17.1 ± 0.6	0.79 ± 0.06	139.2 ± 10.9
OVA/OVA/DEX	0.08 ± 0.05	0.5 ± 0.08	0.6 ± 0.1[b]	1.5 ± 1.4[b]	9.8 ± 0.7[b]	0.59 ± 0.07[b]	102.8 ± 8.2[b]

[a] Value of $p < 0.05$ vs SHAM/PBS/N.CON.
[b] Value of $p < 0.05$ vs OVA/OVA/A.CON.

Lung histopathology

This was performed, as described earlier (20), and microphotographs were taken by Nikon microscope with camera (model YS-100). Slides were numbered randomly and evaluated blindly by two different investigators for the inflammation scoring. Interobserver variation was less than 5%. The quantity of perivascular or peribronchial inflammation was assessed, as described previously, with modifications (23, 24). Briefly, a grade of 0 was assigned when no inflammation was detectable; a grade 1 for occasional cuffing with inflammatory cells; and grades 2, 3, and 4 when most bronchi or vessels were surrounded by a thin layer (1–3 cells), a moderate layer (3–5 cells), and a thick layer (more than 5 cells deep) of inflammatory cells, respectively. An increment of 0.5 was given if the inflammation fell between two grades. Total inflammation score was calculated by addition of both peribronchial and perivascular inflammation scores.

Quantitative morphometry

To quantitate airway mucin content and thickness of epithelium, quantitative morphometry was performed on comparable stained sections from the proximal airways using the freely downloadable ImageJ software version 1.38 (National Institutes of Health, http://rsb.info.hih.gov/ij/). Briefly, stained sections were converted to ×10 digitized images. Using the ImageJ software, images representing the region of interest were split into constituent colors, and threshold was adjusted manually such that only pixels representing a positive stain were seen. Automated particle analysis was used to calculate the pixel area (stain positive area). Pixel length of the basement membrane was calculated separately (circumference). After calibrating pixel length vs actual length in microns, the stain positive area was divided by circumference. After multiplying both the numerator and denominator by 1 mm, it was expressed as vol/mm basement membrane/mm airway length (nl/mm^2).

OVA-specific IgE, IgG1, and IgG2a measurement

Each well of microtiter plate was coated with 2 μg of OVA (IgG1 and IgG2a) and 5 μg of OVA (IgE) (chicken egg OVA grade V; Sigma-Aldrich) in 100 μl vol overnight at 4°C. After three washes, nonspecific sites were blocked with 0.5% Tween 20 in PBS. Mouse sera in duplicate were added to the Ag-coated wells, the plates were incubated, and bound IgE or IgGs were detected with biotinylated anti-mouse IgE, anti-mouse IgG1, or anti-mouse IgG2a (BD Pharmingen). Streptavidin-peroxidase conjugates were added; the bound enzymes were detected by addition of tetramethylbenzidine substrate system (BD Pharmingen); and absorbances were read at 450 nm. Absorbances were converted to arbitrary units.

Isolation of whole lung mitochondria and cytosolic separation

After sacrifice (20), lung portion below the trachea was removed and washed thrice to isolate mitochondria, as described previously (25), with mitochondria isolation kit (Sigma-Aldrich). Briefly, lung portions below the trachea were removed, washed thrice with mitochondrial isolation buffer (isotonic solution containing 10 mM HEPES (pH 7.5), 200 mM mannitol, 70 mM sucrose, and 1 mM EGTA), homogenized in the same buffer containing 2 mg/ml fat-free albumin, and centrifuged at 0°C, 600 × *g* for 6 min. The pellets containing nuclei and debris were discarded, and supernatants were recentrifuged at 11,000 × *g* (first high speed centrifugation) for 12 min. The pellets obtained were reconstituted with isolation buffer and were centrifuged again at 0°C, 600 × *g*, for 6 min. The resultant supernatants were recentrifuged at 11,000 × *g* to get mitochondrial pellets, which were reconstituted with mitochondrial storage buffer (10 mM HEPES (pH 7.4), 250 mM sucrose, 1 mM ATP, 0.08 mM ADP, 5 mM sodium succinate, 2 mM K_2HPO_4, and 1 mM DTT). Cytosolic supernatants resulting from first high speed centrifugation were centrifuged again at 20,000 × *g* for 20 min to get the cytosolic fractions (CYTO). Protein estimation was done for both mitochondrial fractions and CYTO by bicinchoninic acid (Sigma-Aldrich) assay.

Lipid hydroperoxide (L-OOH) and hydroxyoctadecaenoic acid (HODE) assay

Lipid peroxidation was determined in lung tissues by measuring L-OOH with L-OOH assay kit (Cayman Chemical), as per instructions. Briefly, 50 mg of lung tissue was homogenized in 250 μl of PBS and centrifuged at 5000 rpm for 10 min. Resultant supernatant was further used for the extraction of L-OOH with deproteination procedure (Cayman Chemical). Resultant chloroform fractions were used for measurement of L-OOH using Microplate Reader (Bio-Rad), as per instructions. The 13-hydroperoxy octadecadienoic acid was used as the standard. The level of HODE (13-S type) was measured in CYTO by ELISA without extraction (Assay Designs). Briefly, 100 μl of CYTO in duplicate was taken for the measurement by competitive ELISA (13-S-HODE enzyme immunoassay kit from Assay Designs). Results were expressed in ng/100 μg CYTO.

Total cytochrome c *oxidase activity measurement*

COX_{ETC} activity and total citrate synthase activity were measured and calculated, as per instructions (Sigma-Aldrich). Briefly, COX_{ETC} activity was measured based on the oxidation of ferrocytochrome *c* to ferricytochrome *c* by COX_{ETC} present in the mitochondria treated with *n*-dodecyl-β-D-maltoside. This was quantified by the decrease in absorbance at 550 nm. Total citrate synthase activity was measured by the hydrolysis of acetyl CoA to thiols, which reacts with 5′,5′-dithio-bis(2-nitrobenzoic acid) to form 5-thio-2-nitrobenzoic acid. This was detected colormetrically by following the absorption at 405 nm. Positive control experiments were performed with pure cytochrome *c* oxidase or citrate synthase (Sigma-Aldrich). The ratio between total COX_{ETC} and net citrate synthase activities was calculated.

Immunohistochemistry (IHC)

Commercial goat polyclonal Abs for COX_{ETC} subunits II and III (Santa Cruz Biotechnology), mouse mAbs for COX_{ETC} subunit I, and 17-kDa subunit of complex I (Mitosciences and Molecular Probes, respectively) were used as primary Abs, and respective HRP-conjugated secondary Abs (Sigma-Aldrich) were used for IHC (26). Negative control experiments were performed by using either γ-globulin as isotype controls (Jackson ImmunoResearch Laboratories) or omission of primary Abs.

Cytochrome c *estimation*

The levels of cytochrome *c* were measured in CYTO and BAL fluid by ELISA, as per instructions (R&D Systems). Briefly, 5 μg of CYTO protein or 100 μl of BAL fluid supernatants per well in duplicate was used to measure cytochrome *c* with rat/mouse cytochrome *c* enzyme immunoassay kit. For Western blot, cytochrome *c* was separated by 12% SDS-PAGE and transferred onto polyvinylidene difluoride membranes (Millipore). Transferred membrane was blocked with blocking buffer (3% skim milk), incubated with cytochrome *c* Ab (1:2500; Invitrogen), followed by HRP-conjugated anti-mouse secondary Ab, and developed with diaminobenzidine-H_2O_2. α-Tubulin was used as a loading control. Signals were detected by spot densitometry (Alpha EaseFC software from Alpha Innotech).

Table II. *Effects of IL-4 mAb, IFN-γ mAb, and DEX on total, differential, and absolute cells in BAL fluid*[a]

	TCC	Differential count in percentage ($\times 10^4$/ml)				Absolute cells ($\times 10^4$/ml)			
		Macro	Mono	Neutro	Eosino	Macro	Mono	Neutro	Eosino
SHAM/PBS/N.CON	7.5 ± 1.1	77.7 ± 2.8	17.8 ± 3.0	1.9 ± 0.4	0.3 ± 0.2	6.3 ± 0.9	1.0 ± 0.1	1.0 ± 0.6	0.03 ± 0.03
OVA/OVA/A.CON	26.6 ± 2.9[b]	36.9 ± 2.9	17.8 ± 2.8	10.6 ± 2.2	30.1 ± 3.2[b]	11.0 ± 1.4	5.1 ± 1.6	3.8 ± 1.0	7.1 ± 0.9[b]
OVA/OVA/IL-4 mAb	13.9 ± 2.1[c]	48.4 ± 2.1	29.2 ± 10.3	11.1 ± 3.7	11.3 ± 4.5[c]	7.0 ± 1.3	4.2 ± 0.8	1.1 ± 0.6	1.6 ± 0.5[c]
OVA/OVA/IFN-γ mAb	31.0 ± 5.8	41.3 ± 6.2	8.3 ± 5.0	13.9 ± 3.8	26.4 ± 4.0	13.0 ± 2.0	6.2 ± 2.0	4.5 ± 1.3	8.3 ± 1.1
OVA/OVA/DEX	9.0 ± 2.7[c]	50.7 ± 5.0	28.3 ± 5.1	5.7 ± 3.0	15.3 ± 2.9[c]	4.5 ± 1.5	2.0 ± 0.2	0.8 ± 0.6	1.6 ± 0.6[c]

[a] TCC, total cell count; Macro, Macrophage; Mono, mononuclear cells (monocytes and lymphocytes); Neutro, neutrophils; Eosino, eosinophil.
[b] Value of $p < 0.05$ vs SHAM/PBS/N.CON.
[c] Value of $p < 0.05$ vs OVA/OVA/A.CON.

ATP assay

This was done with ATP Bioluminescence Assay kit, as described (Sigma-Aldrich), after TCA extraction. Briefly, 50 mg of weighed tissue was homogenized with 500 μl of 5% TCA and centrifuged at 10,000 × *g* for 20 min at 4°C. The resultant supernatant was optimally diluted with Milli-Q water to estimate the ATP using Bioluminometer (Berthold Technologies), and the amount of bioluminescent signal was recorded and expressed as relative light units.

Statistical analysis

Data are expressed as mean ± SEM. Significant differences between two groups were estimated using unpaired Student's *t* test. Statistical significance was set at $p \leq 0.05$.

Results

OVA-sensitized and challenged mice developed AHR, airway inflammation, mucus hypersecretion, BAL fluid eosinophilia, and increased OVA-specific IgE

As shown in Fig. 2, *A* and *C*, OVA/OVA/A.CON mice have shown MCh dose-dependent increase in Penh and sRaw compared with SHAM/PBS/N.CON mice. In contrast, OVA/OVA/A.CON mice have shown dose-dependent decrease in sGaw (Fig. 2*B*), indicating that OVA-sensitized and challenged mice developed significant AHR. Furthermore, histopathological analysis of lung sections of OVA/OVA/A.CON mice showed dense infiltration of inflammatory cells, including eosinophils in perivascular and peribronchial regions as well as increased mucus secretion and bronchial epithelial hypertrophy (Fig. 3, *A* and *B*; Table I). BAL fluid analysis showed that there was a significant increase in the number of infiltrated cells, including eosinophils, in OVA/OVA/A.CON (Table II). Sera analysis showed a significant increase in the levels of OVA-specific IgE and IgG1 in OVA/OVA/A.CON compared with SHAM/PBS/N.CON mice (Fig. 3*C*). These results indicated that OVA/OVA/A.CON mice developed characteristic features of asthma, such as AHR, airway inflammation, bronchial epithelial hypertrophy, mucus hypersecretion, and increased allergen-specific IgE synthesis.

IL-4 mAb and DEX reduced AHR

To determine the effect of IL-4 on AHR, OVA-sensitized and challenged mice were administered with IL-4 mAb, IFN-γ mAb, or isotypic Ab, and AHRs were determined, as described in *Materials and Methods*. IL-4 mAb administration or DEX treatment attenuated the increase in Penh and sRaw compared with control asthmatic mice (Fig. 2, *A* and *C*). In contrast, the attenuation of the decrease in sGaw was found with IL-4 mAb administration or DEX treatment. In contrast, IFN-γ mAb administration worsened the condition by further increasing the Penh and decreasing sGaw compared with control asthmatic mice. Almost similar results were also obtained in increasing sRaw values (Fig. 2, *B* and *C*).

IL-4 mAb reduced airway inflammation and BAL fluid eosinophilia

To determine the effect of IL-4 on airway inflammation, OVA-sensitized and challenged mice were administered with IL-4 mAb,

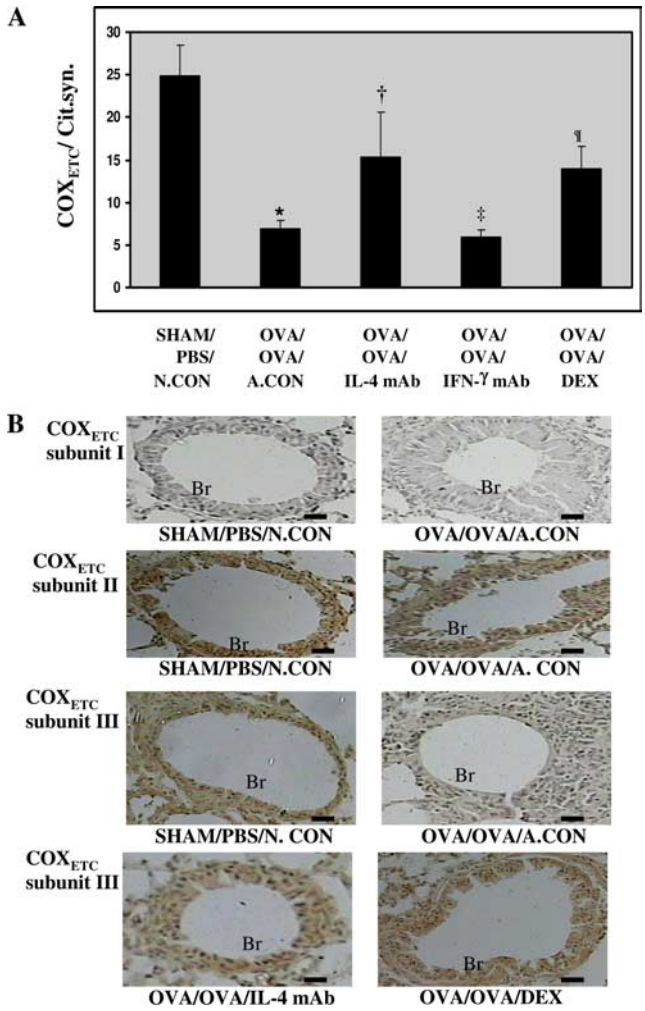

FIGURE 4. IL-4 mAb increased cytochrome *c* oxidase activity. *A*, COX_{ETC} activities were normalized with respective citrate synthase activities. Data were mean ± SEM of three independent experiments. *, $p <$ 0.05 vs SHAM/PBS/N.CON; † and ¶, $p < 0.05$; and ‡, NS vs OVA/OVA/A.CON group. *B*, IHC was done for all mitochondrially coded subunits. *First* and *second panels*, Show the expression of subunits I and II in bronchi, respectively. *Third* and *fourth panels*, Show the expression of subunit III in bronchi. Brown color indicates the positive expression of respective subunit. Br-, Indicates the bronchi. Representative photomicrographs from three independent experiments have been shown. Bars, 50 μm.

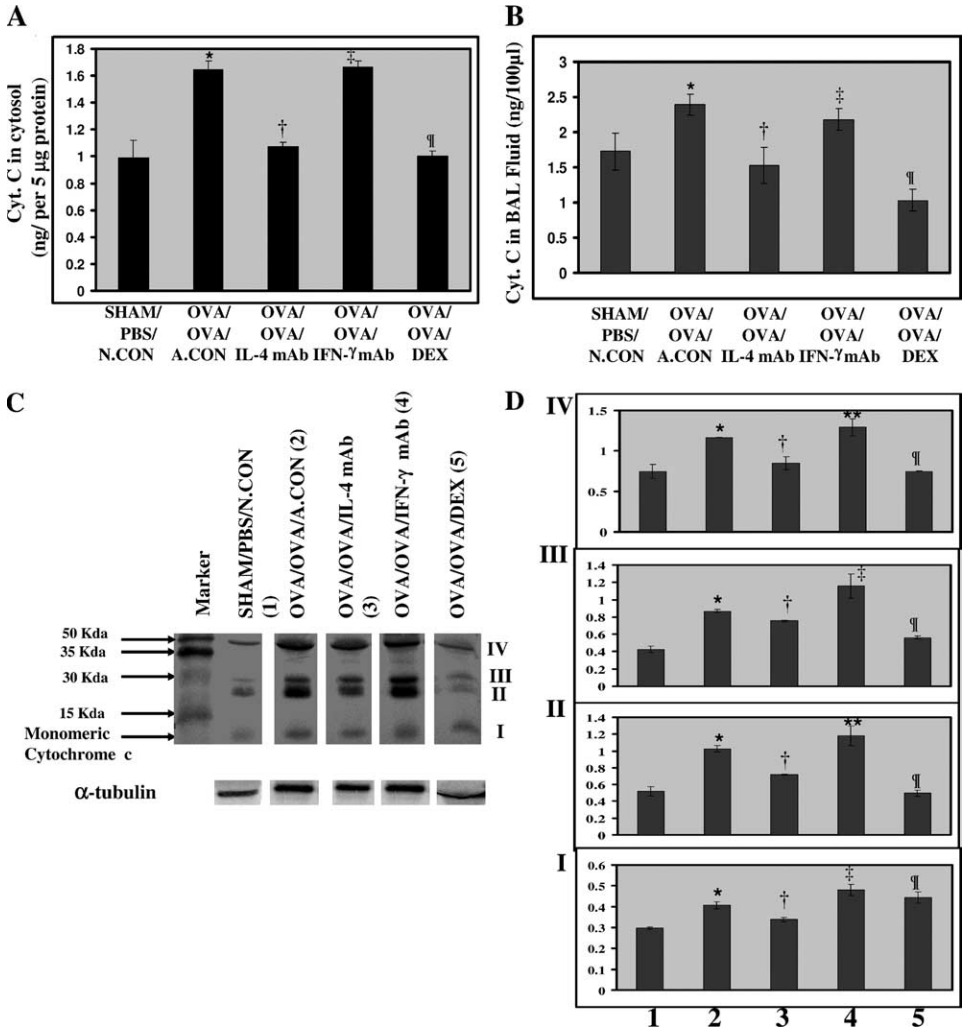

FIGURE 5. IL-4 mAb reduced cytochrome *c* in cytosol and BAL fluid supernatants. *A* and *B*, Cytochrome *c* levels were measured in CYTO, and BAL fluid supernatants by ELISA. Data were mean ± SEM of three independent experiments. ∗, $p < 0.05$ vs SHAM/PBS/N.CON; † and ¶, $p < 0.05$; and ‡, NS vs OVA/OVA/A.CON group. *C*, Cytochrome *c* in CYTO was analyzed by Western blot and compared with α-tubulin (loading control). *D*, Signals were estimated with spot densitometry and divided by respective α-tubulin signals. The results (*A–C*) are shown as a representative of at least three independent experiments. ∗, $p < 0.05$ vs SHAM/PBS/N.CON; † and ‡, $p < 0.05$; and ∗∗, NS vs OVA/OVA/A.CON group.

IFN-γ mAb, or isotypic Ab, and the features of airway inflammation were determined, as described in *Materials and Methods*. Although OVA/OVA/A.CON mice showed dense infiltration of inflammatory cells around the bronchovascular regions along with significant epithelial cell damage, including denudation and/or ulceration of bronchial mucosa, OVA/OVA/IL-4 mAb mice showed focal inflammation around bronchi and vessel, and OVA/OVA/DEX mice showed the features almost similar to N.CON mice. It was also noted that IL-4 mAb or DEX treatment caused least ulceration of epithelium (data not shown) and significant reduction of goblet cell metaplasia (Fig. 3*B*). Also, inflammation score and morphometric analysis showed that OVA/OVA/IL-4 mAb and OVA/OVA/DEX had significant reduction in airway inflammation, airway mucin content, and thickness of bronchial epithelium (Table I). However, OVA/OVA/IFN-γ mAb mice showed features similar to OVA/OVA/A.CON mice (Fig. 3*B*). As shown in Table II, IL-4 mAb or DEX treatment showed the reduction in total cell counts in BAL fluid, as well as absolute numbers of macrophage, neutrophil, and eosinophil.

As IgE class switching is controlled by IL-4 and IFN-γ, OVA-specific IgE levels were measured in sera. As shown in Fig. 3*Ci*, OVA-specific IgE levels were found to be elevated both in OVA/OVA/A.CON and OVA/OVA/IFN-γ. In contrast, it was significantly reduced in OVA/OVA/IL-4 mAb. However, IL-4 mAb did not affect OVA-specific IgG1 levels much (Fig. 3C*ii*). This finding is similar to earlier studies (27), and it could be due to IL-4-independent regulation of IgG1. Interestingly, OVA-specific IgG2a levels were significantly elevated in OVA/OVA/IL-4 mAb compared with OVA/OVA/A.CON (Fig. 3C*iii*).

IL-4 mAb efficiently reduced the L-OOH and HODE

Because airway inflammation produces oxidative microenvironment in the local milieu, we measured the L-OOH levels in the lung tissue and HODE, one of the markers of lipid peroxidation, in the lung cytosol. IL-4 mAb administration significantly reduced the elevated L-OOH and HODE levels (Table I). In contrast, IFN-γ mAb administration did not further increase L-OOH, although HODE levels increased compared with OVA controls.

IL-4 mAb and DEX increased the activity of COX_{ETC}

Because peroxynitrite and NO specifically inhibit COX_{ETC} (8), we measured its activity, and it was normalized by respective citrate synthase activity. The results indicated that the COX_{ETC}/citrate synthase was decreased in OVA/OVA/A.CON mice compared with SHAM/PBS/N.CON (Fig. 4*A*). Interestingly, IL-4 mAb or DEX treatment significantly restored the activity of COX_{ETC}. However, IFN-γ mAb administration decreased the activity further, but it was not statistically significant compared with OVA controls.

IL-4 mAb and DEX restored the reduction in expression of COX_{ETC} subunit III

Because subunits I, II, and III among 13 total subunits of COX_{ETC} are critically important for its activity, IHC was performed for

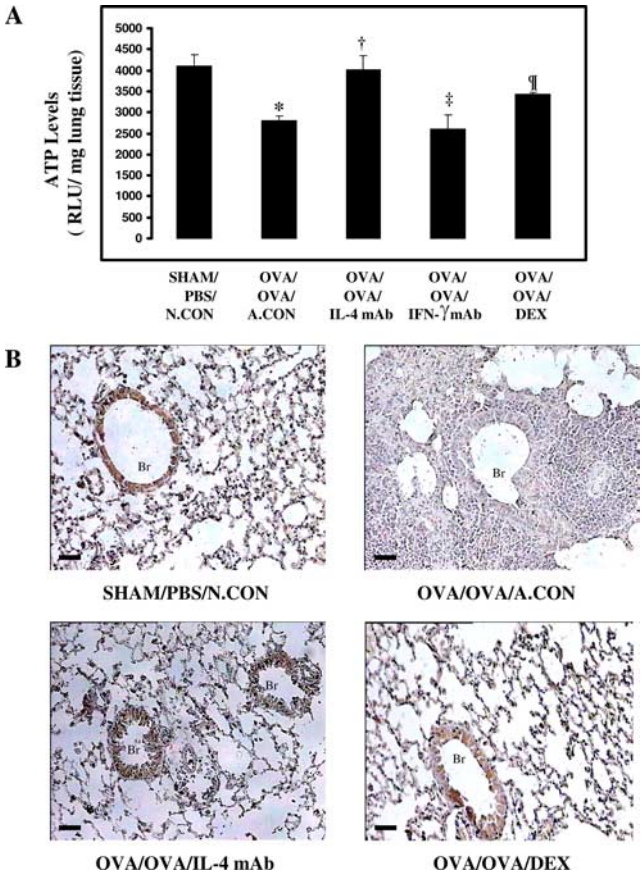

FIGURE 6. IL-4 mAb and DEX restored ATP levels in the lung and the expression of 17-kDa subunit of complex I in bronchial epithelia. *A*, ATP was measured in the lungs after 5% TCA extraction, as described in *Materials and Methods*, and expressed in relative light units/mg lung tissue. *, $p < 0.05$ vs SHAM/PBS/N.CON; † and ¶, $p < 0.05$; and ‡, NS vs OVA/OVA/A.CON group. *B*, IHC was done for 17-kDa subunit of complex I. Br-, Indicates the bronchi. Representative IHC photomicrographs for 17-kDa subunit of complex I. Brown color indicates the positive expression. Br-, Indicates the bronchi. Bars, 100 μm.

these subunits. Subunit I was found to be expressed scarcely in bronchi, and there was no difference between OVA/OVA/A.CON mice and SHAM/PBS/N.CON mice (Fig. 4*B*). In contrast, subunit II was found to be predominantly expressed in bronchi and alveolar epithelial cells compared with other structural cells of the lungs. It was not found to be expressed in infiltrated inflammatory cells. However, no significant difference was observed in its expression in OVA/OVA/A.CON mice compared with SHAM/PBS/N.CON mice. Interestingly, subunit III expression was also found to be predominant in bronchial epithelium and scarcely in alveolar epithelium of SHAM/PBS/N.CON mice, and it was significantly decreased in OVA/OVA/A.CON mice. In contrast, IL-4 mAb or DEX treatment significantly restored the expression.

IL-4 mAb and DEX reduced the appearance of cytochrome c *in cytosol and BAL fluid supernatants*

The reduction in cytochrome *c* oxidase is known to cause the appearance of cytochrome *c* in cytosol (10). We, therefore, analyzed the cytochrome *c* levels by ELISA. The purity of each CYTO was checked by the absence of COX_{ETC} (subunit II) band in Western blot analysis, and also, COX_{ETC} activity was not found to be measurable with 20–25 μg of CYTO (data not shown). As shown in Fig. 5, *A* and *B*, the levels of cytochrome *c* in cytosol and BAL fluid supernatants were significantly increased in OVA/OVA/A.CON or OVA/OVA/IFN-γ mAb mice compared with SHAM/PBS/N.CON mice. Interestingly, IL-4 mAb or DEX treatment showed significant reduction of cytochrome *c* in the cytosol and BAL fluid supernatants. To confirm these results further, we analyzed cytochrome *c* by Western blot (Fig. 5*C*). In OVA/OVA/A.CON and OVA/OVA/IFN-γ mAb mice, 13-kDa band (labeled as "I") was found to be significantly intense compared with SHAM/PBS/N.CON mice, whereas OVA/OVA/IL-4 mAb mice showed a significant reduction of "I" (Fig. 5, *C* and *D*).

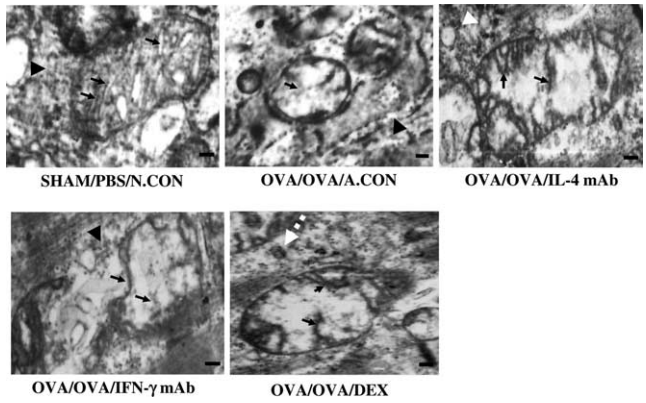

FIGURE 7. IL-4 mAb and DEX restored mitochondrial ultrastructural changes. Transmission electron microscopy was performed, and representative picture from random 50 epithelial cells is shown here from each group. Black arrows, black arrowheads, white broken arrow, and white arrowhead indicate the mitochondrial cristae, rough endoplasmic reticulum, Golgi, and secretary granule, respectively. Bars, 0.1 μm.

Western blot analysis also showed multiple bands other than the 13-kDa band. We have labeled these different forms as II, III, and IV (~26, 30, and 50 kDa, respectively). Interestingly, IL-4 mAb and DEX treatment reduced all multimeric forms (Fig. 5, *C* and *D*). However, IFN-γ mAb administration significantly increased I and III forms compared with OVA/OVA/A.CON mice.

IL-4 mAb and DEX increased ATP levels in the lung

Furthermore, to evaluate one of the vital functions of mitochondria, we measured ATP levels in lung tissue. Interestingly, OVA/OVA/A.CON and OVA/OVA/IFN-γ mAb mice showed significant reduction in ATP levels compared with SHAM/PBS/N.CON mice, and significant reversal of ATP levels was found with IL-4 mAb or DEX treatment (Fig. 6*A*).

IL-4 mAb and DEX restored the reduction in expression of 17-kDa subunit of complex I

Because the ATP levels have been found to be decreased in OVA/OVA/A.CON and the expression of 17-kDa subunit of complex I is related with energy demand (28), IHC was performed for this subunit. We found that this subunit expressed exclusively in the bronchial epithelium of N.CON mice, whereas it was significantly decreased in OVA/OVA/A.CON mice. In contrast, IL-4 mAb treatment significantly restored the expression (Fig. 6*B*).

IL-4 mAb and DEX reduced mitochondrial ultrastructural changes

To evaluate the morphological changes of the mitochondria in bronchial epithelium, we performed transmission electron microscopy; ~50 epithelial cells were visualized randomly from first generation bronchi, and representative photograph of bronchial epithelial mitochondria from each group is shown in Fig. 7. Matrix was dense with tightly packed granules, and well-developed cristae

were seen in mitochondria of SHAM/PBS/N.CON. In contrast, the matrix was less dense with loss of cristae in OVA/OVA/A.CON mice due to the ballooning of mitochondria. Interestingly, when mitochondrial morphology was evaluated after IL-4 mAb or DEX treatment, it significantly restored the mitochondrial structural changes. However, IFN-γ mAb-treated mice showed the features similar to OVA controls.

Discussion

Earlier epidemiologic and genetic evidence suggested that maternal inheritance is one of the substantial risk factors for the development of asthma (29). Mitochondrial haplogroup has been shown to be associated with total serum IgE levels in asthmatics (29). In addition, endogenous reactive oxygen species and/or mitochondrial metabolism has been found to be involved in many phases of immune responses, which are critical in asthma pathogenesis, such as dendritic cell differentiation (30); proliferation of T and B cells; T cell activation; B cell differentiation, which is prerequisite for IgE synthesis; and release of mast cell mediators, including IL-4, which is essential for naive T cell polarization toward Th2 phenotype (29). Thus, mitochondrial oxidative events are thought to be crucial in Ag presentation and in the generation of immune response that may lead to asthma pathogenesis. However, direct demonstration of the involvement of mitochondria in this process is lacking.

In this study, we have shown that mitochondrial dysfunction in experimental allergic asthma is IL-4 dependent. IL-4 is known to cause apoptosis in lung epithelial cells through STAT-6 phosphorylation by up-regulating 15-lipoxygease (12), which has been shown to cause mitochondrial degradation by oxidizing mitochondrial membranes (31). Reduction in the levels of 13-S-HODE and L-OOH by IL-4 mAb (Table I) supports earlier observation that lipid peroxidation is a definite consequence of airway inflammation (2) and is one of the critical prior events for peroxidation of mitochondrial membrane to potentiate its dysfunction (32). HODE is a known lipid oxidative marker in the cytosol, and is one of the peroxide products of linoleic acid, a polyunsaturated fatty acid. Linoleic acid-rich phospholipids such as cardiolipin have a tight physical association with COX_{ETC}, and this association is needed for its maximal activity. Our observations that COX_{ETC} activity was reduced significantly by OVA sensitization and challenge and its activity was restored by treatment with IL-4 mAb or DEX (Fig. 4*A*) suggest that IL-4 is involved in peroxidative damage of cardiolipin in mitochondrial membrane.

Among 13 subunits of COX_{ETC}, the larger and catalytically active subunits (I, II, and III) are coded by mitochondrial DNA, and the remaining 10 subunits are coded by nuclear genes. The role of subunits I and II in electron transfer through binuclear center is well studied, and the role of subunit III in electron transfer is not clear. However, subunit III plays a pivotal role in the assembly and stabilization of the holoenzyme complex, and it is also involved in proton translocation (11). Because mitochondrial subunits are essential for the catalytic activity of the enzyme, expression profile of these three subunits was determined by IHC. There was no difference in the expression of subunits I and II between sham and OVA controls (Fig. 5*B*). However, the expression of subunit III was found to be significantly decreased in OVA controls compared with sham controls. Interestingly, mice treated with IL-4 mAb or DEX have shown increased expression of the subunit III. Our finding supports earlier observation, in which it had been shown that subunit III was primarily decreased during oxidative stress and this decrease was sufficient to cause mitochondrial collapse (11). Therefore, subunit III could be primarily responsible for the reduction of cytochrome *c* oxidase activity in OVA controls. Reduction in COX_{ETC} activity has been observed in many inflammatory oxidative diseases, such as Alzheimer disease and initial stages of diabetes mellitus (33–35). Similar reduction has also been observed along with lipid peroxidation in lymphocytes isolated from tobacco smokers (36). Crucial gaseous proinflammatory molecules such as NO and CO that are involved in the pathogenesis of allergic airway inflammation have been shown to decrease the COX_{ETC} activity (37, 38). Additionally, cytochrome *c* oxidase has tight physical association with cardiolipin, which provides membrane binding sites for cytochrome *c* (39). Therefore, it seems that the interactions among cardiolipin, COX_{ETC}, and cytochrome *c* might create a microenvironment that can modulate structural as well as functional changes in mitochondria. Increased levels of cytochrome *c* levels in A.CON and its reduction by IL-4 mAb or DEX treatment provided evidence to this contention (Fig. 5, *A* and *B*). Interestingly, Western blot analysis showed multimeric forms of cytochrome *c*. This corroborates with earlier findings, which suggested that cytochrome *c* appears in cytosol predominantly in multimeric forms, particularly tetrameric and dimeric forms during apoptosis (40, 41).

Cytochrome *c* oxidase present in inner mitochondrial membrane transfers electron from cytochrome *c* to oxygen to generate transmembrane proton gradient for ATP synthesis, which is one of the vital functions of mitochondria (9). Therefore, ATP levels were measured, and OVA controls showed the significant reduction of ATP levels compared with sham controls, whereas treatment with IL-4 mAb or DEX showed significant restoration (Fig. 6*A*). A significant reduction of 17-kDa subunit of complex I (Fig. 6*B*) along with reduction in ATP levels indicates a possible defect in energy-related functions in bronchial epithelium of OVA-sensitized and challenged mice.

Because bronchial epithelium of OVA controls had shown reduction in the expressions of subunit III of COX_{ETC} and 17-kDa subunit of complex I, it seems that mitochondria of bronchial epithelium is critical in this context. This has been further confirmed by evaluating the morphological changes of the mitochondria in bronchial epithelium (Fig. 7). Also, restoration of mitochondrial damage, such as loss of cristae and ballooning by IL-4 mAb or DEX treatment, but not by IFN-γ mAb, indicates that IL-4 is associated with mitochondrial dysfunction and structural changes in OVA-induced airway inflammation. Thus, IL-4 and mitochondria might build a vicious feedback cycle in the pathogenesis of asthma. However, the molecular mechanism of the involvement of IL-4 in this process remains to be determined in the future. Also, it will be interesting to investigate whether IL-13 may replace IL-4 or whether it may work synergistically with IL-4.

In summary, we demonstrate for the first time that mitochondrial structural alteration and dysfunction are associated with allergic asthma. Thus, our findings may initiate further research on uncovering the role of mitochondria in asthma pathogenesis.

Acknowledgments

The scientific help provided by Dr. Arjun Ram and technical help provided by Tankesh Kumar, Kameshwar Singh, Shashi Kant Singh, Jyotsna Batra, Jyotirmoi Aich, and Neha Gupta are greatly acknowledged. We thank Dr. Anurag Agrawal for his critical comments and suggestions during the preparation and revision of the manuscript, and also for helping us in quantitative morphometry. We also acknowledge the help provided by Sophisticated Analytical Instrument Facility, All India Institute of Medical Sciences, New Delhi.

Disclosures

The authors have no financial conflict of interest.

References

1. Steinke, J. W., and L. Borish. 2001. Th2 cytokines and asthma: interleukin-4: its role in the pathogenesis of asthma, and targeting it for asthma treatment with interleukin-4 receptor antagonists. *Respir. Res.* 2: 66–70.
2. Wood, L. G., P. G. Gibson, and M. L. Garg. 2003. Biomarkers of lipid peroxidation, airway inflammation, and asthma. *Eur. Respir. J.* 21: 177–186.
3. Bucchieri, F., S. M. Puddicombe, J. L. Lordan, A. Richter, D. Buchanan, S. J. Wilson, J. Ward, G. Zummo, P. H. Howarth, R. Djukanovic, et al. 2002. Asthmatic bronchial epithelium is more susceptible to oxidant-induced apoptosis. *Am. J. Respir. Cell Mol. Biol.* 27: 179–185.
4. Truong-Tran, A. Q., D. Grosser, R. E. Ruffin, C. Murgia, and P. D. Zalewski. 2003. Apoptosis in the normal and inflamed airway epithelium: role of zinc in epithelial protection and procaspase-3 regulation. *Biochem. Pharmacol.* 66: 1459–1468.
5. Comhair, S. A., W. Xu, S. Ghosh, F. B. Thunnissen, A. Almasan, W. J. Calhoun, A. J. Janocha, L. Zheng, S. L. Hazen, and S. C. Erzurum. 2005. Superoxide dismutase inactivation in pathophysiology of asthmatic airway remodeling and reactivity. *Am. J. Pathol.* 166: 663–674.
6. Hayashi, T., A. Ishii, S. Nakai, and K. Hasegawa. 2004. Ultrastructure of goblet-cell metaplasia from Clara cell in the allergic asthmatic airway inflammation in a mouse model of asthma in vivo. *Virchows Arch.* 444: 66–73.
7. Konradova, V., C. Copova, B. Sukova, and J. Houstek. 1985. Ultrastructure of the bronchial epithelium in three children with asthma. *Pediatr. Pulmonol.* 1: 182–187.
8. Sharpe, M. A., and C. E. Cooper. 1998. Interactions of peroxynitrite with mitochondrial cytochrome oxidase: catalytic production of nitric oxide and irreversible inhibition of enzyme activity. *J. Biol. Chem.* 273: 30961–30972.
9. Capaldi, R. A. 1992. Structure and function of cytochrome oxidase. *Annu. Rev. Biochem.* 59: 569–596.
10. Hong, M. Y., R. S. Chapkin, R. Barhoumi, R. C. Burghardt, N. D. Turner, C. E. Henderson, L. M. Sanders, Y. Y. Fan, L. A. Davidson, M. E. Murphy, et al. 2002. Fish oil increases mitochondrial phospholipid unsaturation, up-regulating reactive oxygen species and apoptosis in rat colonocytes. *Carcinogenesis* 23: 1919–1925.
11. You, K. R., J. Wen, S. T. Lee, and D. G. Kim. 2002. Cytochrome *c* oxidase subunit III: a molecular marker for *N*-(4-hydroxyphenyl) retinamise-induced oxidative stress in hepatoma cells. *J. Biol. Chem.* 277: 3870–3877.
12. Shankaranarayanan, P., and S. Nigam. 2003. IL-4 induces apoptosis in A549 lung adenocarcinoma cells: evidence for the pivotal role of 15-hydroxyeicosatetraenoic acid binding to activated peroxisome proliferator-activated receptor γ transcription factor. *J. Immunol.* 170: 887–894.
13. Corry, D. B., H. G. Folkesson, M. L. Warnock, D. J. Erle, M. A. Matthay, J. P. Wiener-Kronish, and R. M. Locksley. 1997. Interleukin 4, but not interleukin 5 or eosinophils, is required in a murine model of acute airway hyperreactivity. *J. Exp. Med.* 185: 109–117.
14. Hammad, H., M. Kool, T. Soullié, S. Narumiya, F. Trottein, H. C. Hoogsteden, and B. N. Lambrecht. 2007. Activation of the D prostanoid 1 receptor suppresses asthma by modulation of lung dendritic cell function and induction of regulatory T cells. *J. Exp. Med.* 204: 357–367.
15. Agrawal, A., S. Rengarajan, K. B. Adler, A. Ram, B. Ghosh, M. Fahim, and B. F. Dickey. 2007. Inhibition of mucin secretion with MARCKS-related peptide improves airway obstruction in a mouse model of asthma. *J. Appl. Physiol.* 102: 399–405.
16. Flandre, T. D., P. L. Leroy, and D. J. Desmecht. 2003. Effect of somatic growth, strain, and sex on double-chamber plethysmographic respiratory function values in healthy mice. *J. Appl. Physiol.* 94: 1129–1136.
17. Adler, A., G. Cieslewicz, and C. G. Irvin. 2004. Unrestrained plethysmography is an unreliable measure of airway responsiveness in BALB/c and C57BL/6 mice. *J. Appl. Physiol.* 97: 286–292.
18. Takeda, K., A. Haczku, J. J. Lee, C. G. Irvin, and E. W. Gelfand. 2001. Strain dependence of airway hyperresponsiveness reflects differences in eosinophil localization in the lung. *Am. J. Physiol.* 281: L394–L402.
19. Lofgren, J. L., M. R. Mazan, E. P. Ingenito, K. Lascola, M. Seavey, A. Walsh, and A. M. Hoffman. 2006. Restrained whole body plethysmography for measure of strain-specific and allergen-induced airway responsiveness in conscious mice. *J. Appl. Physiol.* 101: 1495–1505.
20. Ram, A., U. Mabalirajan, M. Das, I. Bhattacharya, A. K. Dinda, S. V. Gangal, and B. Ghosh. 2006. Glycyrrhizin alleviates experimental allergic asthma in mice. *Int. Immunopharmacol.* 6: 1468–1477.
21. McMenamin, P. G. 2000. Optimal methods for preparation and immunostaining of iris, ciliary body, and choroidal wholemounts. *Invest. Ophthalmol. Visual Sci.* 41: 3043–3048.
22. Banerjee, S. K., A. K. Dinda, S. C. Manchanda, and S. K. Maulik. 2002. Chronic garlic administration protects rat heart against oxidative stress induced by ischemic reperfusion injury. *BMC Pharmacol.* 162: 16–24.
23. Jeon, S. G., C. G. Lee, M. H. Oh, E. Y. Chun, Y. S. Gho, S. H. Cho, J. H. Kim, K. U. Min, Y. Y. Kim, Y. K. Kim, and J. A. Elias. 2007. Recombinant basic fibroblast growth factor inhibits the airway hyperresponsiveness, mucus production, and lung inflammation induced by an allergen challenge. *J. Allergy Clin. Immunol.* 119: 831–837.
24. Sur, S., J. S. Wild, B. K. Choudhury, N. Sur, R. Alam, and D. M. Klinman. 1999. Long term prevention of allergic lung inflammation in a mouse model of asthma by CpG oligodeoxynucleotides. *J. Immunol.* 162: 6284–6293.
25. Wu, J. Y., H. J. Kao, S. C. Li, R. Stevens, S. Hillman, D. Millington, and Y. T. Chen. 2004. ENU mutagenesis identifies mice with mitochondrial branched-chain aminotransferase deficiency resembling human maple syrup urine disease. *J. Clin. Invest.* 113: 434–440.
26. Ather, M. H., F. Abbas., N. Faruqui, M. Israr, and S. Pervez. 2004. Expression of pS2 in prostate cancer correlates with grade and chromogranin A expression but not with stage. *BMC Urol.* 4: 14–18.
27. Grunig, G., and V. P. Kurup. 2003. Animal models of allergic bronchopulmonary aspergillosis. *Front. Biosci.* 8: 157–171.
28. Smeitink, J., J. R. Loeffen, R. Smeets, R. Triepels, W. Ruitenbeek, F. Trijbels, and L. van den Heuvel. 1998. Molecular characterization and mutational analysis of the human B17 subunit of the mitochondrial respiratory chain complex I. *Hum. Genet.* 103: 245–250.
29. Raby, B. A., B. Klanderman, A. Murphy, S. Mazza, C. A. Camargo, Jr., E. K. Silverman, and S. T. Weiss. 2007. A common mitochondrial haplogroup is associated with elevated total serum IgE levels. *J. Allergy Clin. Immunol.* 120: 351–358.
30. Del Prete, A., P. Zaccagnino, M. Di Paola, M. Saltarella, C. Oliveros Celis, B. Nico, G. Santoro, and M. Lorusso. 2008. Role of mitochondria and reactive oxygen species in dendritic cell differentiation and functions. *Free Radical Biol. Med.* 44: 1443–1451.
31. Schewe, T. 2002. 15-Lipoxygenase-1: a prooxidant enzyme. *Biol. Chem.* 383: 365–374.
32. Madrigal, J. L., R. Olivenza, M. A. Moro, I. Lizasoain, P. Lorenzo, J. Rodrigo, and J. C. Leza. 2001. Glutathione depletion, lipid peroxidation and mitochondrial dysfunction are induced by chronic stress in rat brain. *Neuropsychopharmacology* 24: 420–429.
33. Maurer, I., S. Zierz, and H. J. Möller. 2000. A selective defect of cytochrome *c* oxidase is present in brain of Alzheimer disease patients. *Neurobiol. Aging* 21: 455–462.
34. Mutisya, E. M., A. C. Bowling, and M. F. Beal. 1994. Cortical cytochrome oxidase activity is reduced in Alzheimer's disease. *J. Neurochem.* 63: 2179–2184.
35. Trigulova, V. S. 1978. Cytochrome oxidase activity in diabetes mellitus. *Probl. Endokrinol.* 24: 14–16.
36. Miró, O., J. R. Alonso, D. Jarreta, J. Casademont, A. Urbano-Márquez, and F. Cardellach. 1999. Smoking disturbs mitochondrial respiratory chain function and enhances lipid peroxidation on human circulating lymphocytes. *Carcinogenesis* 20: 1331–1336.
37. Mason, M. G., P. Nicholls, M. T. Wilson, and C. E. Cooper. 2006. Nitric oxide inhibition of respiration involves both competitive (heme) and noncompetitive (copper) binding to cytochrome *c* oxidase. *Proc. Natl. Acad. Sci. USA* 103: 708–713.
38. D'Amico, G., F. Lam, T. Hagen, and S. Moncada. 2006. Inhibition of cellular respiration by endogenously produced carbon monoxide. *J. Cell Sci.* 119: 2291–2298.
39. Robinson, N. C. 1993. Functional binding of cardiolipin to cytochrome *c* oxidase. *J. Bioenerg. Biomembr.* 25: 153–163.
40. Loretta, D., S. Read, D. Cakouros, J. R. Huh, B. A. Hay, and S. Kumar. 2002. The role of cytochrome *c* in caspase activation in *Drosophila melanogaster* cells. *J. Cell Biol.* 156: 1089–1098.
41. Balk, J., and C. J. Leaver. 2001. The PET1-CMS mitochondrial mutation in sunflower is associated with premature programmed cell death and cytochrome *c* release. *Plant Cell* 13: 1803–1818.